

Understanding hydrological processes with scarce data in a mountain environment

A. Chaponnière,^{1*} G. Boulet,² A. Chehbouni² and M. Aresmouk³

¹ International Water Management Institute-West Africa, Accra, Ghana

² IRD-CESBIO (UMR 5126 CNES-CNRS-UPS-IRD), Toulouse, France

³ Agence de Bassin du Haouz-Tensift, Marrakech, Morocco

Abstract:

Performance of process-based hydrological models is usually assessed through comparison between simulated and measured streamflow. Although necessary, this analysis is not sufficient to estimate the quality and realism of the modelling since streamflow integrates all processes of the water cycle, including intermediate production or redistribution processes such as snowmelt or groundwater flow. Assessing the performance of hydrological models in simulating accurately intermediate processes is often difficult and requires heavy experimental investments. In this study, conceptual hydrological modelling (using SWAT) of a semi-arid mountainous watershed in the High Atlas in Morocco is attempted. Our objective is to analyse whether good intermediate processes simulation is reached when global-satisfying streamflow simulation is possible. First, parameters presenting intercorrelation issues are identified: from the soil, the groundwater and, to a lesser extent, from the snow. Second, methodologies are developed to retrieve information from accessible intermediate hydrological processes. A geochemical method is used to quantify the contribution of a superficial and a deep reservoir to streamflow. It is shown that, for this specific process, the model formalism is not adapted to our study area and thus leads to poor simulation results. A remote-sensing methodology is proposed to retrieve the snow surfaces. Comparison with the simulation shows that this process can be satisfyingly simulated by the model. The multidisciplinary approach adopted in this study, although supported by the hydrological community, is still uncommon. Copyright © 2007 John Wiley & Sons, Ltd.

KEY WORDS hydrological modelling; intermediate processes; equifinality issues; SWAT; geochemical signature; snow coverage

Received 11 July 2006; Accepted 20 March 2007

INTRODUCTION

Mountainous regions concentrate more than half of the Earth's fresh water (Klemes, ●1990; Rodda, 1994; Weingartner *et al.*, 2003). In the current context of global environmental degradation and climate change, preservation of this fragile environment is a high priority and requires a good understanding of the different physical processes that affect the dynamics of these complex systems. This was the main objective of the SUDMED project, where this study is situated (Chehbouni *et al.* 2006). However, the hydrology of mountainous areas is poorly known: Klemes (●1990) qualifies it as 'the blackest of the water cycle's black boxes'. Observation networks are often very limited, even though their density should be higher than what is available in the floodplains in order to capture the high variability in space and time of the water fluxes.

Thanks to the High Atlas range, the semi-arid regions of the south of Morocco receive a significant amount of precipitation that sustains both agriculture and urbanization (Schulz and de Jong, 2004). However, whereas water demand is increasing due to demographic pressure, water resources are expected to decrease in both quality and quantity due to environmental changes. Appropriate hydrological modelling is thus required to understand

the dominant processes controlling the water balance in the basin so that local authorities can be provided with science-based elements to carry out decisions on the management of water resources. This study focuses on a head-watershed (227 km²) in the Central High Atlas, for which a large proportion of the precipitation falls as snow from November to April. Understanding the hydrology of head watersheds, the supplying zone, is a first step towards improved water management; but it is also a challenge, since many possible transfer mechanisms can be activated in these watersheds: evapotranspiration, surface runoff, subsurface runoff, groundwater flow, and snow dynamics.

Because of the harsh observation conditions of most mountain environments, gathering information through a combination of remote sensing, ground measurements, geographical information systems (GISs) and models is a necessity. If many improvements have been made through the growing availability of remote-sensing data, selecting a model adapted to mountain hydrology remains a challenge. For instance, Krishna (2005) combined remote-sensing images, GIS techniques and ground measures to assess the snow and glacier cover in the Himalayas. For mountainous catchment-scale hydrological modelling, Holko and Lepistö (1997) used TOP-MODEL in Slovakia. The limitations of their modelling performance were due to their assumption of a homogeneous soil profile and inadequate snow subroutine.

* Correspondence to: A. Chaponnière, IWMI-West Africa, PMB CT 112, Cantonments, Accra, Ghana. E-mail: a.chaponniere@cgiar.org

1 Andréassian *et al.* (2004) used two simple, continu- 60
 2 ous, lumped watershed models (GR4J, a four-parameter 61
 3 model, and TOPMO, an eight-parameter modified 62
 4 version of TOPMODEL) on 62 watersheds in France. Both 63
 5 lumped models give good results, but they cannot provide 64
 6 any insight into the different intermediate processes. To 65
 7 learn more about the streamflow-generation mechanisms 66
 8 in the Western Ghats region (mountains located in South 67
 9 India), Putty and Prasad (2000) used a lumped concep- 68
 10 tual model based on the variable source-area theory. The 69
 11 results show that flow from dynamic subsurface saturated 70
 12 zones contributes substantially to quickflow: fieldwork 71
 13 and a modified version of the model were necessary. 72
 14 Globally, as stated by Winiger *et al.* (2005), the combina- 73
 15 tion of remote-sensing techniques and runoff models can 74
 16 potentially lead to a better understanding of the mountain 75
 17 hydrology; but this is not straightforward, as an adapta- 76
 18 tion to the region of interest is required. 77

19 Because the main characteristic of mountain environ- 78
 20 nments is their complexity, one would be tempted to 79
 21 choose a detailed, physically based model to represent its 80
 22 water cycle. But much more information than what can 81
 23 be reasonably available is required to implement such a 82
 24 distributed conceptual hydrological model. This certainly 83
 25 leads to overparameterization and the need for calibra- 84
 26 tion. When conceptual rather than lumped modelling is 85
 27 used, special attention has to be paid to the calibration 86
 28 process, since a better fit does not always mean that the 87
 29 model represents the reality of the processes. This prob- 88
 30 lem is amplified over complex watersheds, where almost 89
 31 all hydrological processes (superficial runoff, groundwa- 90
 32 ter contribution, evapotranspiration, snowmelt, etc.) can 91
 33 occur simultaneously and their impacts on streamflow 92
 34 are space–time-scale dependent. In this context, the key 93
 35 questions are: 94

- 36 1. Does a good simulated streamflow guarantee a realistic 95
 37 representation of intermediate water balance processes 96
 38 including storage terms (e.g. snowmelt) and lateral 97
 39 flow redistribution (e.g. groundwater flow)? 98
 40
- 41 2. How can we get insight into processes without very 99
 42 intensive fieldwork? In other words, is it possible to 100
 43 develop a limited measurement strategy of some key 101
 44 variables that ensures proper assessment of the water 102
 45 balance components? 103
 46

47 In this study, we first address the issue of parameter 104
 48 intercorrelation in the context of conceptual hydrological 105
 49 modelling over a semi-arid mountainous watershed. Then 106
 50 attempts are made to address the realism and accuracy 107
 51 of the simulated components of the water cycle, such 108
 52 as groundwater flow and snow-cover depletion, once the 109
 53 model had been calibrated against observed streamflow 110
 54 only. 111

55 The main scope of this paper is to demonstrate that 112
 56 comparing the observed and the simulated streamflow 113
 57 is not sufficient to validate a conceptual spatially distributed 114
 58 hydrological model: intermediate processes have to be 115
 59 analysed, since compensation effects on the resulting 116
 117

118 outlet flow can be important. Obtaining good modelling 60
 61 results for the wrong reasons is, indeed, a well-known 62
 63 problem in the modelling community (Beven and Quinn, 64
 1994; Batchelor *et al.*, 1998; Andréassian *et al.*, 2004). 65
 In this context, the underlying question is whether 66
 correct global streamflow restitution can coincide with 67
 incorrectly simulated intermediate processes. 68

This paper is organized as follows: we first present the 69
 object of our study, the Rheraya watershed in the central 70
 region of Morocco. We then briefly describe the dis- 71
 tributed conceptual model used to assess the hydrological 72
 cycle of this catchment, the Soil and Water Assessment 73
 Tool (SWAT; Arnold *et al.*, 1993). In the third section, 74
 the model performance is analysed in terms of streamflow 75
 simulation and the problem of parameter intercorrelation 76
 is identified throughout the optimization process. In the 77
 fourth section we analyse the methodology and instru- 78
 mentation developed to characterize two intermediate 79
 processes, namely the deep drainage and the contribu- 80
 tion of snowmelt to streamflow. Finally, the results and 81
 the approach are discussed with respect to the objectives 82
 and questions raised above. 83

84 SITE LOCATION AND AVAILABLE DATA 85

86 The Haouz Plain in south-central Morocco is made up 87
 88 of several intensively irrigated districts and is fed by 89
 nine head-watersheds located in the High Atlas range. 90
 The Atlas range and the Haouz Plain belong to a 91
 larger watershed called the Tensift watershed covering 92
 20 450 km² (see Figure 1). This region is characterized 93
 by scarce water resources and is subject to frequent 94
 drought. 95

96 The study took place in one of the nine Atlasic head 97
 98 watersheds: the Rheraya catchment. This head watershed 99
 covers a surface area of about 227 km² and is charac- 100
 101 terized by a semi-arid and mountainous climate. Indeed, 102
 the mean measured annual precipitation at the outlet was 103
 363 mm for the period 1971–2002 and the closest meteo- 104
 105 rological station registered a mean annual potential evap- 106
 107 otranspiration of 1816 mm from a Colorado pan for the 108
 period 1984–2001. The watershed altitude ranges from 109
 1084 to 4167 m, precipitation occurring as snow in the 110
 upper parts of the watershed. The main geological forma- 111
 tion is granite, but there are some clay inclusions present 112
 north of the watershed, as well as limestone-marl forma- 113
 tions. Overall, the bedrock is shallow and fractured. 114
 In terms of geomorphology, rock faces and scree slopes, 115
 debris fans and gravelly riverbeds are found. Slopes are 116
 very steep, with an average grade of 19%, and soils are 117
 shallow. Based on these features, quick flow response 118
 is expected in this basin: its concentration time, esti-
 mated from geometric and geomorphological data, is 4 h.
 Figure 2 presents the mean monthly rainfall and stream-
 flow data at the watershed's outlet between 1971 and
 2002. Rainfall and streamflow data are characterized by
 high inter- and intra-annual variability, which is typical
 of semi-arid areas. The average streamflow is 19.3 mm

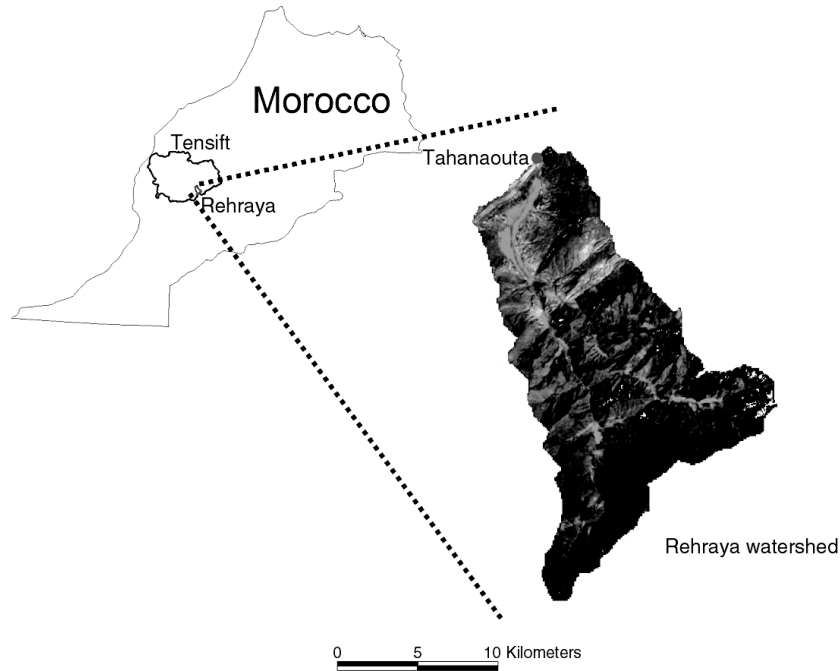


Figure 1. The Tensift watershed situated in southern Morocco and the Rehraya subwatershed situated south of the Tensift watershed, in the Atlas mountain range. Tahanaouta, the outlet of the watershed, is located north of the Rehraya

1 month⁻¹, which represents 1.67 m³ s⁻¹. A 2- to 3-month shift is observed between the pattern of annual rainfall and that of streamflow. This delay characterizes slow flow processes, which can be caused by the existence of different geomorphological units as well as an important groundwater and/or snow component in the water balance.

8 The Rehraya watershed is thus a complex terrain in which many hydrological processes are likely to be involved: surface runoff on the steep slopes and shallow soils under convective rainfall events, shallow subsurface flow in the fractured bedrock, high evaporation rates under semi-arid climatic conditions, slow processes due to snowmelt and/or to groundwater flow. Also, few data are available: the only measurements are streamflow and rainfall collected at the outlet (Tahanaouta, see Figure 1), which are insufficient to provide insight into the hydrological processes occurring in the watershed.

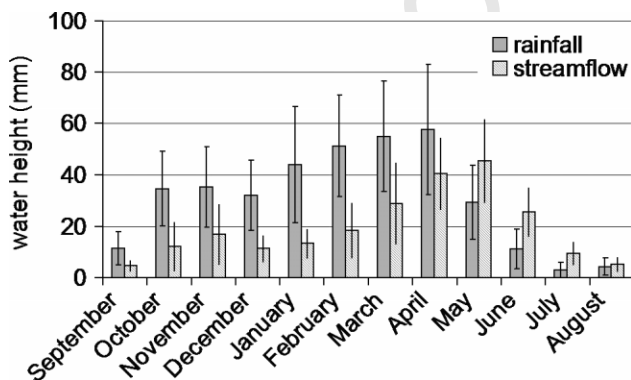


Figure 2. Mean monthly precipitation (mm) and streamflow (m³ s⁻¹) and standard deviation at the outlet of the Rehraya watershed on the period 1971–2002

Precipitation in a semi-arid mountainous watershed, as in most other mountain watersheds, is spatially and temporally highly variable (Tani, 1996; Holko and Lepistö, 1997; Weingartner *et al.*, 2003; Krishna, 2005; Winiger *et al.*, 2005). Figure 2 presents the temporal variability of precipitation and streamflow at the watershed's outlet. One can see that the standard deviation is of the same order of magnitude as the mean, which indicates the complexity of the basin. As a result of the watershed morphology (high elevation gradient and the coexistence of different climatic influences: semi-continental from the north, oceanic from the west and Saharan from the south), significant spatial variations of precipitation exist. The preliminary analysis of the data collected for a rain-gauge network installed in the watershed in 2003–2004 shows that annual precipitation (from 1 April 2003 to 1 April 2004) varies from 241 mm to 562 mm across the watershed (see Chaponnière (2005)). Since only one rain-gauge is available before 2003, it is necessary to select years during which this rain-gauge is representative of the rainfall events occurring over the whole watershed; if not, hydrological modelling should not be attempted, since modelling results depend on the quality of input data (Holko and Lepistö, 1997). We assume that a good correlation between the timing of peak flow and rainfall throughout the year attests that the outlet rain-gauge has been representative of the events that occurred in the watershed.

THE SOIL AND WATER ASSESSMENT TOOL

Based on the climatic and topographical characteristics of the Rehraya watershed combined with the poor data set, we chose a model that accounted for most of

1 the hydrological processes while maintaining a simple
 2 approach for each of them. Based on a comprehensive
 3 literature review, SWAT (Arnold *et al.*, 1993) turned out
 4 to be most suitable.

5 SWAT was developed to assess the impact of land-use
 6 and climate changes on water balance at the watershed
 7 scale. It operates at a daily time step, is physically
 8 based, spatially distributed and takes into account a large
 9 number of processes. SWAT has been extensively used
 10 and validated at various spatial and temporal scales.
 11 Hernandez *et al.* (2000) and Muttiah and Wurbs (2002)
 12 proved the validity of streamflow simulation under semi-
 13 arid climates, and Arnold and Allen (1996) demonstrated
 14 the validity of major hydrological processes on three
 15 Illinois watersheds.

16 The elementary spatial unit of the model is the
 17 hydrological response unit (HRU), which is defined by
 18 a unique combination of geology, land use and soil
 19 type in a given subbasin. Figure 3 illustrates the way
 20 the hydrological cycle is simulated by SWAT on each
 21 HRU; the processes are calculated sequentially. Major
 22 inputs for the model are topography, land use, soil type,
 23

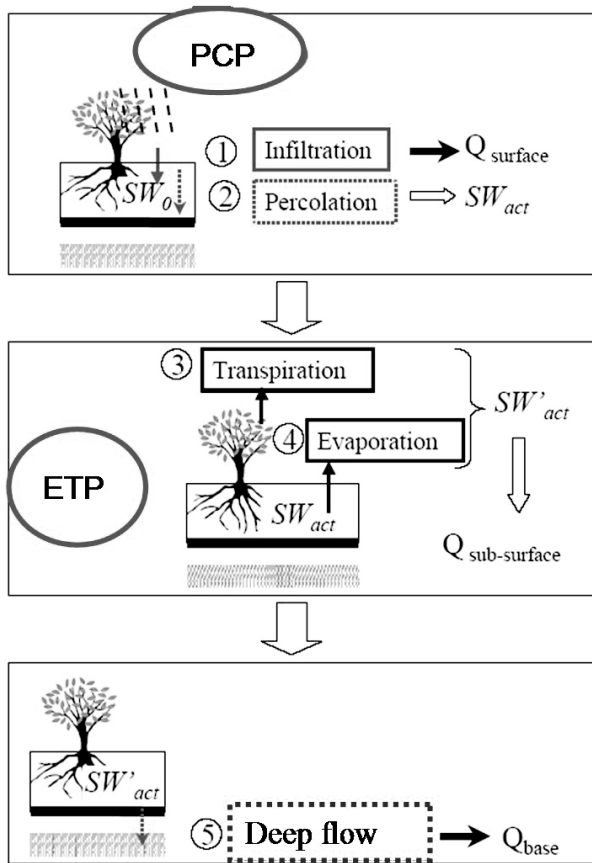


Figure 3. SWAT's modelling scheme for the water balance. Initial soil water is known (SW_0). During a rainfall event (PCP), infiltration (1) and percolation (2) are the two processes simulated first: surface runoff $Q_{surface}$ is then established and soil water actualized (SW_{act}). A second step consists in calculating transpiration (3) and evaporation (4) fluxes in response to the atmospheric evapotranspiration demand (potential evapotranspiration or ETP). Soil water is updated (SW'_{act}) and subsurface runoff is calculated ($Q_{subsurface}$). Finally, the updated soil water provides the percolation flux towards the deep reservoir and the contribution of this reservoir to the streamflow (Q_{base})

groundwater characteristics and climatic data. Outputs are
 available at different spatial scales, namely the HRU, the
 subbasins and the basin; they mainly consist of water
 fluxes (evapotranspiration, surface runoff, infiltration,
 lateral runoff, percolation, streamflow in the stream
 network, etc.) and vegetation variables (yield, root water
 uptake, etc.).

Following an intensive sensitivity analysis (see
 Chaponnière (2005)), eight model parameters were
 selected: the altitudinal gradients for precipitation and
 temperature (spatialization of the climatic data set), the
 soil depth and available water capacity, the delay coeffi-
 cient for groundwater and subsurface flow, a parameter
 used to convert snow water equivalent into snow cover-
 age (parameter 'cov₂' in Equation (4)) and the snowfall
 temperature. These parameters will be calibrated in the
 following section.

When implementing the model on the Rehraya water-
 shed we took into account three HRUs based on geo-
 morphological *in situ* observations and soil and geologi-
 cal maps (see Figure 4): one unit is the valley bottom
 (referred to as 'soil 2'), characterized by deep soil with
 a texture dominated by sand (the river bed is gravel) and
 clay and the main land cover is a dense agricultural veg-
 etation; the second unit is located in the upper part of the
 watershed ('soil 1a') and is made up of bare shallow and
 sandy soil; the third unit ('soil 1b') is in the lower part
 of the watershed and is characterized by intermediate shal-
 low soil with a loamy sand texture and sparse trees (pines
 and juniper). All soils are considered to be constituted of
 a single layer. Once the spatial distribution of the HRU
 is taken into account, 12 parameters must be calibrated.

STREAMFLOW MODELLING PERFORMANCE AND IDENTIFICATION OF INTERCORRELATED PARAMETERS

The accuracy of the routinely available hydrological data
 is questionable: precipitation observations are rarely rep-
 resentative of the whole catchment, and streamflow itself
 is subject to measurement errors. Streamflow at the outlet
 is calculated on the basis of the measured water depth and

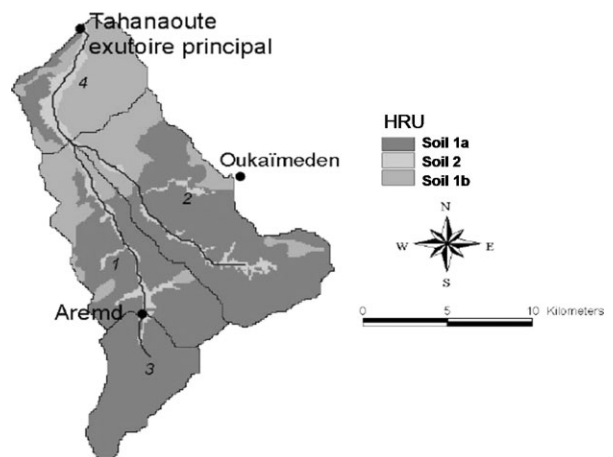


Figure 4. HRU distribution on the Rehraya watershed

1 the stage–discharge rating curve. In semi-arid and moun- 60
 2 tainous areas, intense convective rainfall events cause 61
 3 significant fluvial erosion and deposits. The streambed 62
 4 is frequently modified, and this affects the rating curve. 63
 5 Rating curves are valid for several years under stable 64
 6 environmental conditions, but must be updated several 65
 7 times a year in the Rehraya watershed. Rating curve 66
 8 updating is an expensive and time-consuming task when 67
 9 done so frequently, and the hydrological services in the 68
 10 Tensift watershed have to monitor a large number of sta- 69
 11 tions under these conditions. Consequently, rating curves 70
 12 are not always updated and streamflow measurements are 71
 13 thus subject to errors. We analysed streamflow measure- 72
 14 ments and corrected them when possible to allow reliable 73
 15 time-series. 74

16 To ensure that rainfall events are representative of 75
 17 the whole catchment, we selected hydrological years for 76
 18 which there is a good correlation between peak flow 77
 19 and precipitation at the outlet. The years 1980–1981 to 78
 20 1983–1984, 1990–1991 to 1998–1999 and 2001–2002 79
 21 were considered. 80

22 Streamflow data at the outlet is an important measure 81
 23 since it integrates all the hydrological processes active 82
 24 in the watershed (Winiger *et al.*, 2005). It is also the 83
 25 most commonly available data. As a consequence, model 84
 26 calibration is generally achieved by minimizing the dis- 85
 27 tance between the measured and the simulated stream- 86
 28 flow estimates. In this study, calibration is carried out by 87
 29 maximizing the Nash and Sutcliffe efficiency (Nash and 88
 30 Sutcliffe, 1970), which is defined by 89

$$31 \text{Eff} = 1 - \frac{\sum_i^N (\text{obs}_i - \text{sim}_i)^2}{\sum_i^N (\text{obs}_i - \text{obs}_{my})^2} \quad (1)$$

32 where i is the time-step, N is the total number of 90
 33 simulated time-steps, obs_i is the observation at time-step 91
 34 i , sim_i is the simulation at time-step i and obs_{my} is the 92
 35 mean of the observations for the simulated period. 93
 36 94
 37 95

38 When implementing a distributed conceptual hydrolog- 96
 39 ical model, uncertainty can come from different sources 97
 40 (Pellenq and Boulet, 2004): boundary conditions, initial 98
 41 conditions, model parameters, forcing variables, and 99
 42 model formulation. Concerning the parameters, available 100
 43 data are mostly insufficient to reduce this uncertainty (e.g. 101
 44 uncertainty in the parameters' spatio-temporal distribu- 102
 45 tion and their representative means; uncertainty in the 103
 46 value of the parameters themselves). When the degree of 104
 47 freedom of the simulation is higher than the degree of 105
 48 constraints (defined by all the available observations) the 106
 49 observation system is underdetermined or overparameter- 107
 50 ized (Ambroise, 1999). Overparameterization is common 108
 51 when distributed conceptual models are used. Through 109
 52 model optimization, the issue of overparameterization is 110
 53 linked with the issue of parameter intercorrelation and 111
 54 parameter dependence. Two parameters are fully inde- 112
 55 pendent if the optimal value obtained for one parameter 113
 56 is independent from that of the other parameter. On the 114
 57 other hand, when two parameters are correlated, the same 115
 58 model output can be simulated with different combina- 116
 59 tions of these parameters. This means that a large number 117
 of solutions represented by best-fit couples of parameters 118

is independent from that of the other parameter. On the 60
 other hand, when two parameters are correlated, the same 61
 model output can be simulated with different combina- 62
 tions of these parameters. This means that a large number 63
 of solutions represented by best-fit couples of parameters 64
 are obtained when this output is used to compute the cost 65
 function. Under these conditions, improvement of model 66
 performance is as likely to result from parameter inter- 67
 correlation (existence of many best-fit realistic values) 68
 as from any improvement of the representation of physi- 69
 cal processes (Batchelor *et al.*, 1998). Indeed, Beven and 70
 Quinn (1994) showed that a wide range of parameter 71
 sets can be fitted so that models are able to reproduce 72
 observed data. This has been termed the 'equifinality' 73
 issue (Beven, 1996). Consequently, in order to assess the 74
 hydrological modelling performance, several of the pro- 75
 cesses involved should be analysed individually and not 76
 just the resulting streamflow. Moreover, priority should 77
 be given to the analysis of processes that are simulated 78
 using parameters for which intercorrelation issues have 79
 been identified. However, investigating the performance 80
 of the model in terms of intermediate processes is often 81
 difficult and requires skilled staff and costly equipment 82
 that are not available, especially in developing countries. 83
 In fact, model outputs represent processes that are con- 84
 trolled by physical properties which vary in both time 85
 and space. Apart from discharge data, which integrates 86
 basin-scale processes, most of the other measurements 87
 (such as soil moisture, leaf area index, evapotranspira- 88
 tion, groundwater recharge, etc.) represent instantaneous 89
 physical properties at a single point/grid. Different solu- 90
 tions have been suggested in the literature to overcome 91
 this scale problem. Regarding soil moisture, for exam- 92
 ple, Schmutge and Jackson (1996) show that the simple 93
 mean of soil moisture values can be sufficient over flat 94
 terrain, and most workers place high hopes on remote- 95
 sensing techniques that can provide either large-scale 96
 area-average values (passive microwave) or spatially dis- 97
 tributed fine-scale values (active microwave). Despite the 98
 existence of techniques such as high spatio-temporal res- 99
 olution satellite sensors and large-aperture scintillometers 100
 (Chehbouni *et al.*, 2000; Ezzahar *et al.*, 2007), which 101
 give access to the spatial and temporal distributions of the 102
 process, their implementation remains confined to very 103
 specific studies and teams. Most hydrological studies do 104
 not have the required budget and skills to implement such 105
 instrumentation and rely on more classical measurement 106
 devices, which brings us back to the calibration issue and 107
 its associated problems. 108

The problem of parameter intercorrelation can be iden- 109
 tified by analysing best-fit parameter ranges when one, 110
 two or more parameters are tuned to reduce the difference 111
 between the simulated and the observed daily stream- 112
 flow. If the optimal values of one particular parameter 113
 are within the same range no matter how many param- 114
 eters are calibrated, then this parameter is not subject to 115
 intercorrelation. However, if the optimal values are scat- 116
 tered or if the optimal range changes when the number of 117
 tuned parameters increases, then intercorrelation should 118

1 be expected. Sorooshian and Gupta (1983) identify three
 2 sources of equifinality issues during calibration: (1) the
 3 structure of the model, (2) the inadequacy of the model
 4 in representing reality and (3) the data and its associated
 5 measurement or scaling error. We have already mentioned
 6 issues related to the third source of equifinality. In the
 7 following sections we focus on the first two factors.

8 During the calibration period, a good simulation perfor-
 9 mance can be achieved with SWAT (see Figure 5: a
 10 Nash efficiency of 0.83 is obtained). The good-fit val-
 11 ues (values of the parameter that produce 80% of the
 12 global maximum efficiency) were analysed throughout
 13 the calibration of an increasing number of parameters.
 14 As stated above, the range of best-fit parameters during
 15 successive calibrations is a good illustration of parameter
 16 intercorrelation. Behaviours of pairs of parameters along
 17 the successive calibrations are displayed in Figures 6–8.
 18 Figure 6 presents the altitudinal gradient of precipitation
 19 on the x -axis ('gdt pcp'), the altitudinal gradient of tem-
 20 perature on the y -axis ('gdt tmp') and the Nash efficiency
 21 on the z -axis ('efficiency'). Each point represents a good-
 22 fit simulation: a specific combination of both gradients
 23 leads to an efficiency greater than 80% of the maximum
 24 efficiency. In the first graph ('opt 2p') only two paramet-
 25 ers are calibrated (the two gradients), whereas additional
 26 parameters are calibrated in the following graphs (three
 27 'opt3p', four 'opt4p' up to 8 'opt8p'). Altogether, up to
 28 12 parameters have been calibrated, but not all graphs
 29 are displayed here. We analysed the consequence of the
 30 calibration of these additional parameters on the values
 31 obtained for the altitudinal gradients. In Figures 7 and 8,
 32 the same representation is adopted for different paramet-
 33 ers. In Figure 7, the depth of one soil type (referred
 34 to as 'Depth(soil1a)') is reported on the x -axis of the
 35 graphs located on the left part of the figure and the
 36 depth of another soil ('Depth(soil2)') is reported on the
 37 x -axis of the graphs located on the right-hand side of
 38 the figure. On the y -axis the depth of the third soil type
 39 ('Depth(soil1b)') is reported on all graphs. In Figure 8,
 40 the x -axis displays the value of the groundwater delay
 41 (referred as 'Gw delay') whereas the y -axis displays the
 42 value of the snowfall temperature T_{snowfall} .

43 To identify possible intercorrelation issues, one can
 44 interpret the extent of the good-fit parameter space.
 45 The three figures show different behaviours: in Figure 6
 46 the scatter plot occupies a very limited space; when
 47 the fifth parameter is calibrated, the range of possible
 48 values increases, but the cluster of points is centred
 49 around the same space as when only four parameters
 50 are tuned. Altitudinal gradients of temperature and pre-
 51 cipitation do not seem to be subject to intercorrelation.
 52 However, in Figures 7 and 8, the scatter is much more
 53 important and remains so throughout the successive cali-
 54 brations. Different parameters have been analysed fol-
 55 lowing the same approach: the parameters related to the
 56 soil compartment—such as soil depth (see Figure 7) and
 57 available water capacity (not shown), to groundwater (see
 58 groundwater delay in Figure 8) and, to a lesser extent,
 59 snow modules (see Figure 8)—all show a large scatter

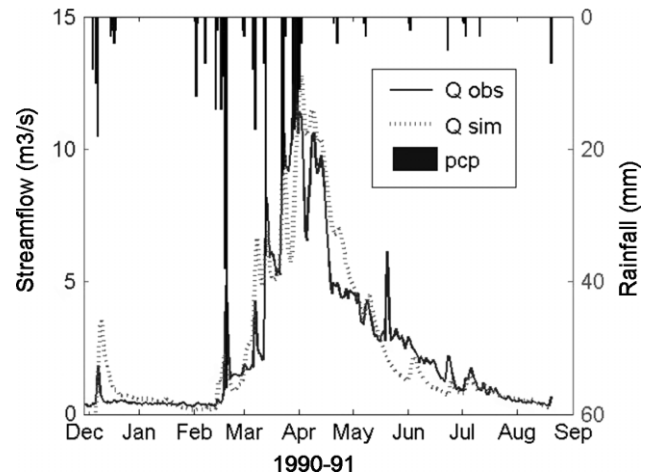


Figure 5. Simulated (dashed line) and measured (thick line) streamflow ($\text{m}^3 \text{s}^{-1}$) together with precipitation (mm) for year 1990–1991

of points in the two-parameter space and, thus, evidence
 of potential intercorrelation. Given the lack of avail-
 able observation tools for this compartment, at least at
 the catchment scale, subsurface water transfer has not
 been addressed in this study. Concerning the groundwa-
 ter and snow modules, geochemistry and remotely sensed
 data have been used to understand the processes and
 make direct comparison between the modelled and mea-
 sured processes. How close to 'reality' are the simulated
 intermediate processes? We attempt to answer this ques-
 tion in the next sections, alongside a description of the
 tools and methodologies specifically used or developed
 to answer it.

In what follows, the calibrated parameters are set
 according to the calibration exercise and remain
 unchanged. After calibration, a validation exercise was
 performed for various hydrological years displaying con-
 trasting hydrological conditions. Table I presents the
 mean streamflow and simulation performance (the cor-
 relation coefficient, the Nash efficiency and the root-
 mean-square error (RMSE)) for the six selected years.
 The mean streamflow ranges from $0.64 \text{ m}^3 \text{ s}^{-1}$ to
 $1.83 \text{ m}^3 \text{ s}^{-1}$. Correlation coefficients range from 0.43 to
 0.75, but the Nash efficiencies are mostly negative. This
 demonstrates a poor simulation performance. Figure 9a
 presents precipitation together with the measured and
 simulated streamflow for the years 1981–1982. The sim-
 ulation reproduces the seasonal pattern of streamflow
 fairly well (correlation coefficient 0.64), but some major
 events are missing at the beginning and at the end of the
 simulation period. This explains the negative Nash effi-
 ciency (-0.12) and the high RMSE ($2.09 \text{ m}^3 \text{ s}^{-1}$) of that
 particular year. Figure 9b presents the simulated stream-
 flow and the measured precipitation and streamflow for
 1995. The simulated hydrograph, although reproducing
 the shape satisfactorily (correlation coefficient 0.59), is
 shifted by about 1 month: the high flow period begins
 and ends 1 month earlier in the simulation compared with
 the observations. With no major peak flows missing through-
 out the simulation, the Nash efficiency is positive (0.11).
 In both cases we observe poor modelling performance for

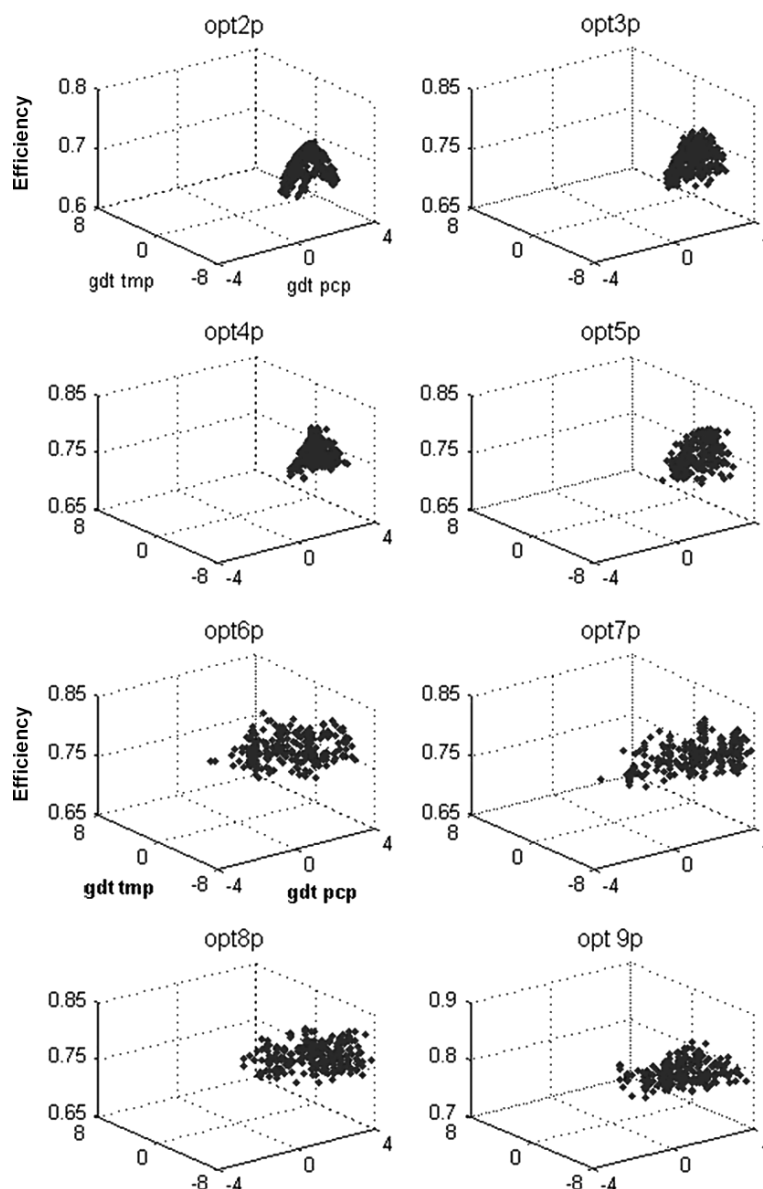


Figure 6. Values of temperature ('gdt tmp') and precipitation ('gdt pcp') altitudinal gradients leading to a modelling performance higher or equal to 80% of the maximum efficiency when 2, 3, until 12 parameters are calibrated

Color Figure - Online only

1 different reasons (either peak flows omitted or a 1-month
 2 shift). Semi-arid mountainous environments face extreme
 3 spatial variability of meteorological conditions that cannot
 4 be taken into account if an appropriate observation
 5 network is not available. The hydrological community
 6 should put considerable effort into developing observation
 7 networks, but this remains a difficult and expensive
 8 task rarely fulfilled by national hydrology services, especially
 9 in developing countries.

11 INTERMEDIATE PROCESSES: METHODOLOGY
 12 AND RESULTS

14 *Geochemical analysis of groundwater contribution to
 15 streamflow*

16 *Methodology.* A river's geochemical signature gives
 17 some information on the origin of its water. Its composition
 18 depends on the reservoir it originates from (whether
 19

Table I. Simulation criteria (correlation coefficient, Nash efficiency and RMSE) obtained on validation years

Year	Correlation coefficient	Nash efficiency	RMSE (m ³ s ⁻¹)	Mean streamflow (m ³ s ⁻¹)
1980–1981	0.43	-0.07	1.42	1.18
1981–1982	0.64	-0.12	2.09	1.25
1983–1984	0.75	-0.53	1.30	0.64
1993–1994	0.43	-1.19	3.65	1.83
1995	0.59	0.11	1.23	1.33
1996–1997	0.66	-7.34	2.72	0.88

it is the surface, subsurface or deep reservoir). Geochemical sampling can thus be used to identify the contributing reservoirs during a flood and to quantify their relative contribution to annual streamflow. In this

20
 21
 22
 23
 24
 25
 26
 27
 28
 29
 30

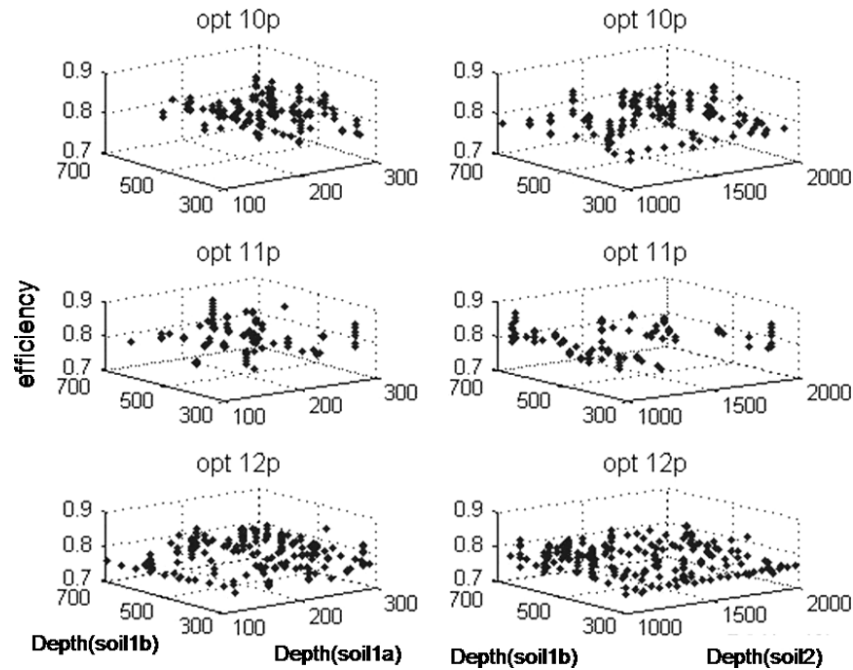


Figure 7. Values of soil depth ('Depth(soil1b)', 'Depth(soil1a)', 'Depth(soil 2)') leading to a modelling performance higher or equal to 80% of the maximum efficiency

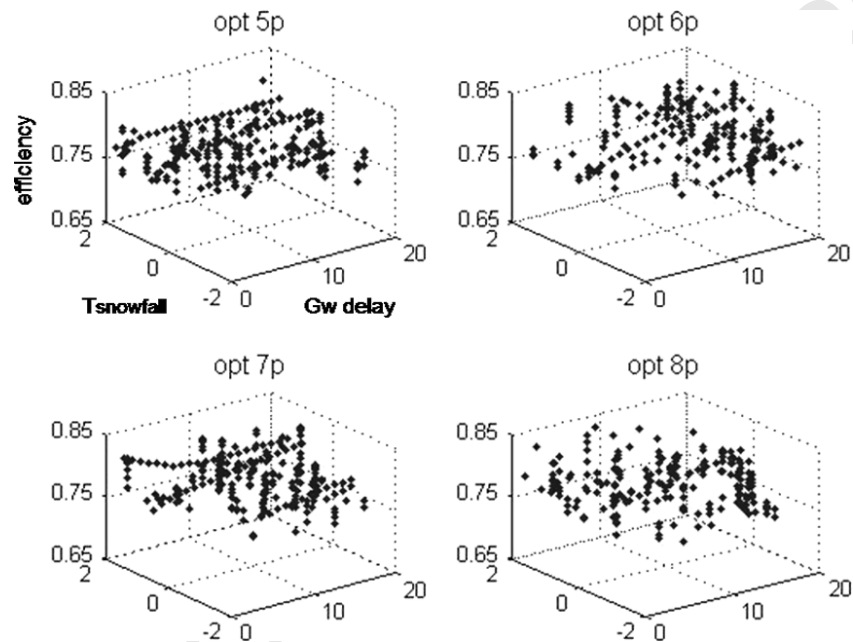


Figure 8. Values of snowfall temperature T_{snowfall} and groundwater delay ('Gw delay') leading to a modelling performance higher or equal to 80% of the maximum efficiency

1 study, we analysed the silica and dissolved organic carbon (DOC) content of water with respect to streamflow. 12
 2 These two elements were chosen for two reasons. First, reservoirs respectively. Water coming from deep reservoirs 13
 3 they are not significantly influenced by atmospheric contamination, since precipitation contains almost no silica and low DOC concentrations, whereas water coming from the superficial 14
 4 they are not significantly influenced by atmospheric contamination, since precipitation contains almost no silica or DOC (Probst *et al.*, 1990). Second, they have different origins (Idir *et al.*, 1999; Tardy *et al.*, 2004): whereas water coming from the superficial 15
 5 they are not significantly influenced by atmospheric contamination, since precipitation contains almost no silica or DOC (Probst *et al.*, 1990). Second, they have different origins (Idir *et al.*, 1999; Tardy *et al.*, 2004): whereas water coming from the superficial 16
 6 they are not significantly influenced by atmospheric contamination, since precipitation contains almost no silica or DOC (Probst *et al.*, 1990). Second, they have different origins (Idir *et al.*, 1999; Tardy *et al.*, 2004): whereas water coming from the superficial 17
 7 they are not significantly influenced by atmospheric contamination, since precipitation contains almost no silica or DOC (Probst *et al.*, 1990). Second, they have different origins (Idir *et al.*, 1999; Tardy *et al.*, 2004): whereas water coming from the superficial 18
 8 they are not significantly influenced by atmospheric contamination, since precipitation contains almost no silica or DOC (Probst *et al.*, 1990). Second, they have different origins (Idir *et al.*, 1999; Tardy *et al.*, 2004): whereas water coming from the superficial 19
 9 they are not significantly influenced by atmospheric contamination, since precipitation contains almost no silica or DOC (Probst *et al.*, 1990). Second, they have different origins (Idir *et al.*, 1999; Tardy *et al.*, 2004): whereas water coming from the superficial 20
 10 they are not significantly influenced by atmospheric contamination, since precipitation contains almost no silica or DOC (Probst *et al.*, 1990). Second, they have different origins (Idir *et al.*, 1999; Tardy *et al.*, 2004): whereas water coming from the superficial 21
 11 they are not significantly influenced by atmospheric contamination, since precipitation contains almost no silica or DOC (Probst *et al.*, 1990). Second, they have different origins (Idir *et al.*, 1999; Tardy *et al.*, 2004): whereas water coming from the superficial 22

1 of the different reservoirs can be related to streamflow,
 2 which has to be measured continuously. The method
 3 determines, at each sampling time t , the individual con-
 4 tribution $Q_k(t)$ ($m^3 s^{-1}$) of each reservoir k to the total
 5 streamflow $Q_t(t)$ ($m^3 s^{-1}$) as specified by Equation (2).
 6 The main assumption of the method is that the contribu-
 7 tion of the different reservoirs (from 1 to k) changes with
 8 time independently of its geochemical characteristics (C_k^i
 9 is the concentration in geochemical element i of reservoir
 10 k) (see Equation (3)):

$$Q_t(t) = \sum_{k=1}^K Q_k(t) \quad (2)$$

$$Q_t^i(t)C_t^i(t) = \sum_{k=1}^K C_k^i Q_k^i(t) \quad (3)$$

11
 12
 13
 14
 15
 16
 17
 18 Water samples were collected on a fortnightly basis
 19 at the outlet of the watershed from April to December
 20 2003. Common assumptions are that the contribution of
 21 the superficial reservoir is dominant during the high flow
 22 period (Probst, 1992), whereas the deep reservoir is the
 23 only one contributing to streamflow during the low flow
 24 period (Smakhtin, 2001). The geochemical composition
 25 of each reservoir can thus be directly characterized by
 26 the geochemical signature of streamflow at these specific
 27 periods of time. Once the geochemical composition of
 28 the reservoir is known, the relative contribution of each
 29 reservoir can be calculated at each sampling time and then
 30 extended throughout the year by establishing a relation
 31 between the contribution of one reservoir and the total
 32 streamflow. This method reveals the contribution of deep
 33 and superficial reservoirs to streamflow. In the following
 34 section, these contributions were compared with the deep
 35 reservoir contribution simulated by the SWAT.

36
 37 **Results.** The geochemical compositions of both reser-
 38 voirs are displayed in Table II. The superficial reservoir
 39 is characterized by a high DOC content and low silica
 40 content, whereas the deep reservoir presents the inverse
 41 geochemical signature. The linear regression established
 42 to estimate the contribution on a continuous basis is pre-
 43 sented in Figure 10. Consequently, the reservoirs' con-
 44 tributions to streamflow were identified and plotted in
 45 Figure 11. The deep reservoir contribution (thick line)
 46 is very stable and equal to the summer streamflow. The
 47 superficial reservoir (diamond symbols) shapes the hydro-
 48 graph. The partition of the contributions is consistent with
 49 the basin features, i.e. a steep mountainous watershed
 50 with shallow soils. The geochemical measures show that
 51 the deep reservoir contribution could be simulated as a
 52 constant value throughout the year.

53 SWAT simulations of groundwater contribution to
 54 streamflow present consistent patterns from one year to
 55 the next (see Figure 12a–c). Very little groundwater con-
 56 tribution is simulated during low flow period, but it
 57 increases slightly during high flow period. The ground-
 58 water contribution to streamflow is expressed in SWAT
 59 as an increasing function of an average soil water content

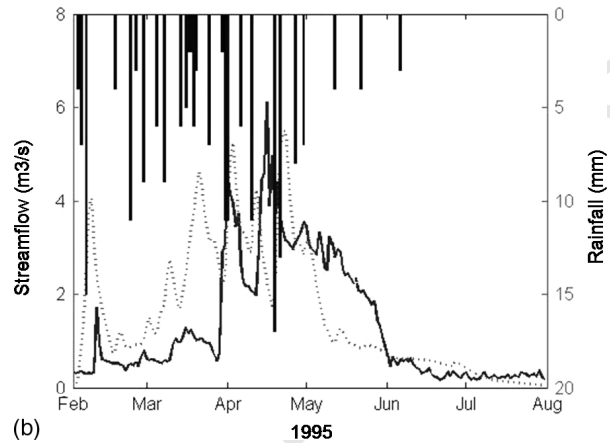
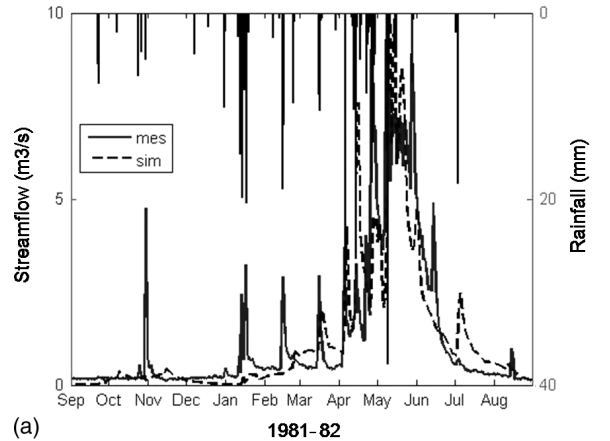


Figure 9. Simulated (dashed line) and measured (thick line) streamflow ($m^3 s^{-1}$) together with precipitation (mm) for (a) year 1981–1982 and (b) 1995

Table II. Geochemical profile (●silica and DOC) of both reservoirs

	●Si (ppm)	DOC (mg l ⁻¹)
Superficial reservoir	4.57	2.69
Deep reservoir	5.89	0.87

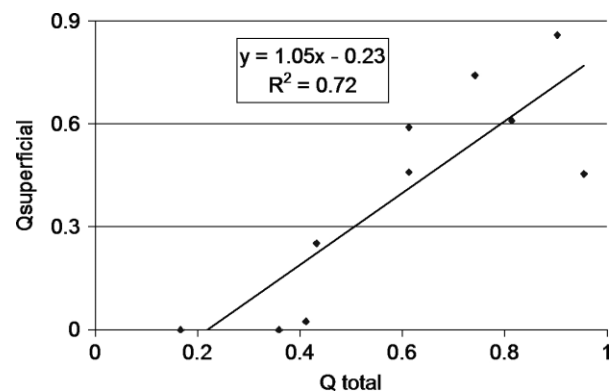


Figure 10. Linear relationship between total streamflow Q_{total} and streamflow from the superficial reservoir $Q_{superficial}$ established from point measurements in order to define $Q_{superficial}$ throughout the year

with a proportionality factor; in our example it follows the streamflow signal pattern with no contribution from

Color Figure - Online only

AQ4

AQ3

Color Figure - Online only

60
 61
 62
 63
 64
 65
 66
 67

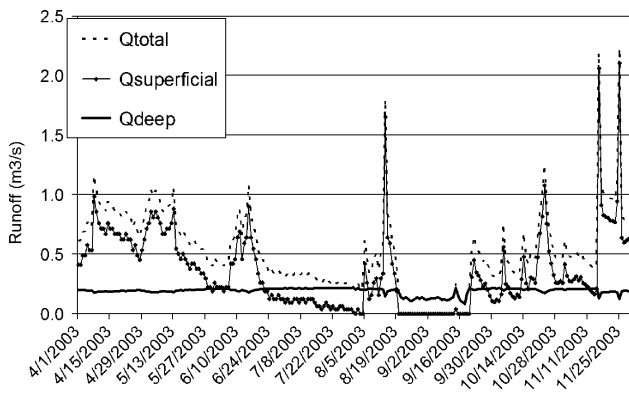


Figure 11. Rehraya watershed hydrograph ($\text{m}^3 \text{s}^{-1}$) between April and December 2003. The total streamflow is represented by a dashed line, the superficial reservoir contribution to streamflow is represented by diamonds and the groundwater reservoir contribution is represented by a thick line

constant groundwater release with a strict application of an average Darcy-like equation. Other workers (Sophocleous and Koelliker, 1999; Conan *et al.*, 2003) reported similar conclusions in different climatic and geographical conditions.

Remote sensing for snow surface identification

Methodology. As mentioned earlier, the watershed culminates at 4167 m. Each year, snow covers the upper parts of the basin. There is no snow cover monitoring network on the site. Implementing one would represent significant investment due to the remoteness of the region and the cost of installing snow-water-equivalent measuring devices or snow-height monitoring stations. Remote sensing is thus a useful tool for snow surface monitoring in high mountainous areas where field instrumentation is difficult to implement and expensive to maintain. In semi-arid mountainous zones, where snowmelt dynamics are very rapid (see Schulz and de Jong (2004: figure 4)) and the terrain is highly heterogeneous (slope and aspect, vegetation cover and types), sensors presenting a high temporal frequency and high spatial resolution are required. However, such sensors do not yet exist. To overcome this difficulty, we developed a method combining high-resolution (Landsat-TM images, 30 m resolution) and low-resolution (SPOT-VEGETATION images, 1 km resolution) satellite images (Chaponnière *et al.*, 2005). This method establishes a relationship between the snow index at low resolution and the snow surface derived from the classification of high-resolution images. In this research, a new snow index specifically

1 summer to December. In some cases, though, what is
 2 simulated is a small increase in late winter and gener-
 3 ally a gradual increase in spring followed by gradual
 4 decrease 1 or 2 months later. Overall, however, the sim-
 5 ulated groundwater contribution is small, since the soils
 6 are shallow and exhibit a very low water storage capacity.
 7 This pattern is not consistent with the results from geo-
 8 chemical analysis. The formulation adopted by SWAT's
 9 groundwater module is thus not appropriate for the char-
 10 acteristics of the mountainous watershed under investi-
 11 gation: even if the amplitude of the groundwater signal
 12 were to increase through increased soil storage capacity,
 13 it would remain mathematically impossible to simulate a

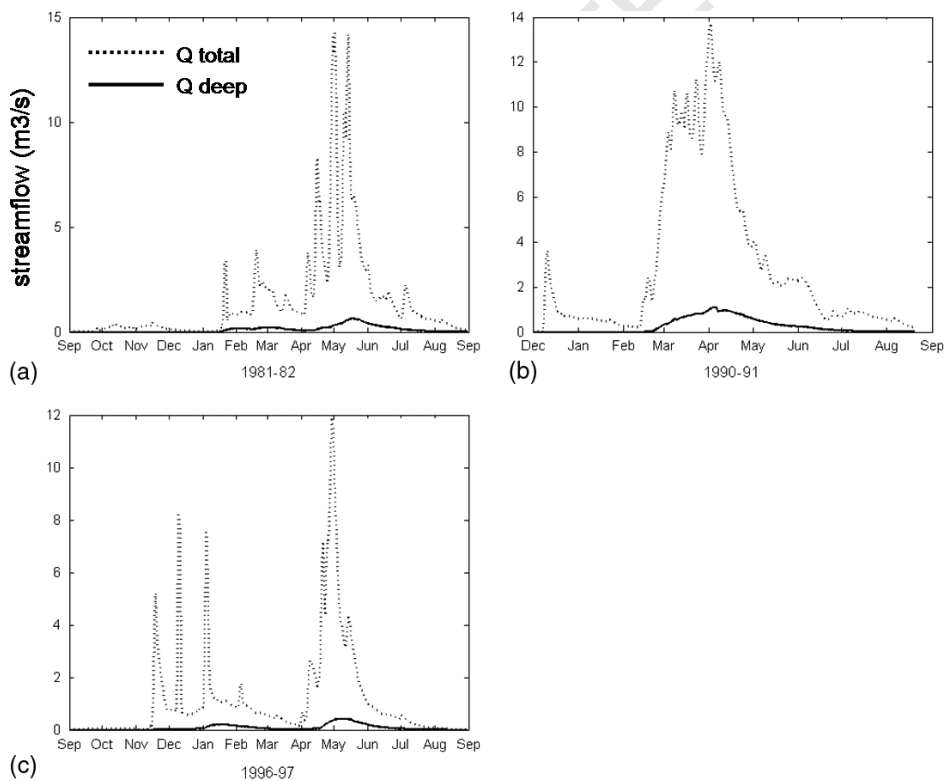


Figure 12. Total streamflow (dashed line) and groundwater streamflow (thick line) simulated with the SWAT model for (a) year 1981–1982, (b) year 1990–1991 and (c) year 1996–1997

Color Figure - Online only

1 adapted to the Atlas Mountains was developed. It corrects for the influence of the soil spectral signature/noise
 2 in the original snow index. However, information on
 3 snow depth cannot be retrieved from these wave-
 4 lengths. The main limitations of the methodology are
 5 (see Chaponnière *et al.* (2005)) the coarse spatial res-
 6 olution of the images (1 km), the high scatter of low
 7 values in the index-to-area relationship and the tem-
 8 poral intervals of the low-resolution images (SPOT-
 9 VEGETATION), which are often longer than 1 or 2 days.
 10 As a consequence, uncertainty in the snow surface esti-
 11 mates is difficult to quantify. The features related to snow
 12 cover dynamics that can be estimated with the highest
 13 degree of confidence with coarse-resolution satellite data
 14 are (i) the start and end dates for the snow season and
 15 (ii) the maximum values of snow cover during the sea-
 16 son. In the next section the temporal profiles obtained
 17 from satellite imagery will be compared with the profiles
 18 simulated by the SWAT model.
 19

20
 21 **Results.** Time-series covering the hydrological years
 22 1998–1999 to 2001–2002 were processed with the
 23 above-mentioned remote-sensing methodology (see
 24 Chaponnière *et al.* (2005) for details). The snow cover
 25 (in square kilometres) over the basin obtained from satel-
 26 lite images (SPOT-VEGETATION) was considered as
 27 the reference (or ‘ground truth’) but was subject to a
 28 large number of uncertainties, as stated above. The data
 29 were compared with the snow cover simulated by SWAT
 30 to investigate how the model is able to reproduce this
 31 secondary process. In SWAT, the snow water equivalent
 32 SNO for a given HRU is converted to snow surface sno_{cov}
 33 •via

$$sno_{cov} = \frac{SNO}{SNO_{100}} \left[\frac{SNO}{SNO_{100}} + \exp \left(cov_1 - cov_2 \frac{SNO}{SNO_{100}} \right) \right]^{-1} \quad (4)$$

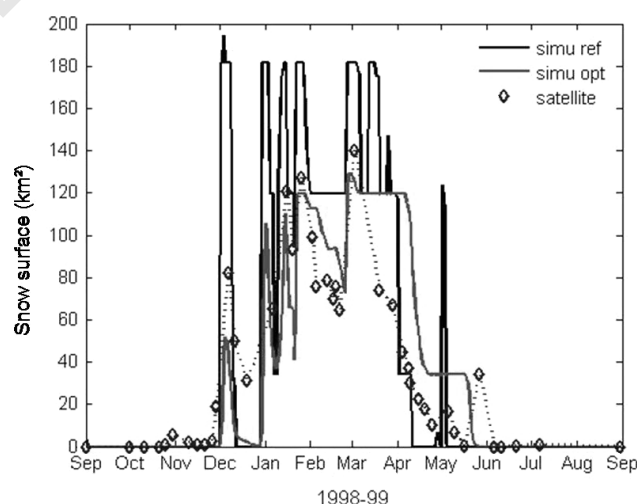
34
 35
 36
 37
 38
 39
 40 where SNO_{100} is the threshold snow water equivalent
 41 for which 100% coverage is reached and cov_1 and cov_2
 42 design the shape of the curve that characterizes the
 43 distribution of snow within the HRU. The SNO_{100} value
 44 depends on factors such as vegetation distribution, wind
 45 effects, interception and aspect. Once the volume of water
 46 held in the snowpack exceeds SNO_{100} , the depth of snow
 47 over the HRU is assumed to be uniform, i.e. $sno_{cov} = 1.0$.
 48 The areal depletion curve affects snowmelt only when
 49 the snowpack water content is between 0.0 and SNO_{100} .
 50 Consequently, the impact of the areal depletion curve
 51 on snowmelt depends on the SNO_{100} value. Modification
 52 of SNO_{100} (from the default value to a measured or
 53 calibrated value) greatly influences snow dynamics.

54 For the year 1998–1999, this sno_{cov} parameter was
 55 calibrated (‘simu opt’ on Figure 13) to fit the observed
 56 snow cover. Figure 13 shows time-series of snow cover
 57 simulated by SWAT using the default parameter of the
 58 snow-distribution equation (‘simu ref’, continuous line)
 59 and simulation with the calibrated parameter (‘simu opt’,

60 dashed line) and satellite observation (‘satellite’, diamond
 61 symbols). As far as the seasonal pattern is concerned
 62 (snow accumulation, maximum cover and snow disap-
 63 pearance periods), both simulations are close to satellite
 64 observations. Snow surface is present from early Decem-
 65 ber to late June. Despite differences between the simu-
 66 lated and the observed time-series in the calibration
 67 data set, the calibration of the snow distribution equation
 68 improved the results in terms of simulated snow surface
 69 and dynamics. The calibrated equation was then applied
 70 for the additional time-series in the validation data set.
 71 Figure 14a–c shows simulated snow cover using either
 72 calibrated or default parameters, as well as satellite obser-
 73 vation for years 1999–2000, 2000–2001 and 2001–2002,
 74 these three years representing our validation data set.

75 The calibrated equation shows an overall satisfying fit
 76 with all observations and a significant improvement com-
 77 pared with the default equation in terms of estimated
 78 snow surface and timing of snowfall and snowmelt.
 79 We thus conclude that the formalism adopted in SWAT
 80 for the simulation of snow cover dynamics is appropri-
 81 ate for our watershed. Of course, important differences
 82 remain between simulated and satellite-retrieved snow
 83 cover temporal profiles for the reasons presented above
 84 (uncertainty of ‘observation’ and simplicity of simula-
 85 tion).

86 The correlation between the remotely sensed snow
 87 cover and SWAT’s outputs presents some limitations.
 88 Indeed, some snowfall events are not simulated at all
 89 (the first and last events in Figure 13, the last events
 90 in Figure 14a and b, the first event in Figure 14c) due
 91 either to an unobserved precipitation event in the rainfall
 92 data set or to high generated atmospheric temperature
 93 preventing rainfall from falling as snow. Also, the
 94 typical decline of snow cover is not well reproduced
 95 in the model, especially in the spring time. The model
 96 presents a scale-shaped curve characteristic of models
 97 using thresholds. This is the case for SWAT’s snow
 98
 99



100
 101
 102
 103
 104
 105
 106
 107
 108
 109
 110
 111
 112
 113
 114
 115
 116
 117
 118
 119
 120
 121
 122
 123
 124
 125
 126
 127
 128
 129
 130
 131
 132
 133
 134
 135
 136
 137
 138
 139
 140
 141
 142
 143
 144
 145
 146
 147
 148
 149
 150
 151
 152
 153
 154
 155
 156
 157
 158
 159
 160
 161
 162
 163
 164
 165
 166
 167
 168
 169
 170
 171
 172
 173
 174
 175
 176
 177
 178
 179
 180
 181
 182
 183
 184
 185
 186
 187
 188
 189
 190
 191
 192
 193
 194
 195
 196
 197
 198
 199
 200
 201
 202
 203
 204
 205
 206
 207
 208
 209
 210
 211
 212
 213
 214
 215
 216
 217
 218
 219
 220
 221
 222
 223
 224
 225
 226
 227
 228
 229
 230
 231
 232
 233
 234
 235
 236
 237
 238
 239
 240
 241
 242
 243
 244
 245
 246
 247
 248
 249
 250
 251
 252
 253
 254
 255
 256
 257
 258
 259
 260
 261
 262
 263
 264
 265
 266
 267
 268
 269
 270
 271
 272
 273
 274
 275
 276
 277
 278
 279
 280
 281
 282
 283
 284
 285
 286
 287
 288
 289
 290
 291
 292
 293
 294
 295
 296
 297
 298
 299
 300
 301
 302
 303
 304
 305
 306
 307
 308
 309
 310
 311
 312
 313
 314
 315
 316
 317
 318
 319
 320
 321
 322
 323
 324
 325
 326
 327
 328
 329
 330
 331
 332
 333
 334
 335
 336
 337
 338
 339
 340
 341
 342
 343
 344
 345
 346
 347
 348
 349
 350
 351
 352
 353
 354
 355
 356
 357
 358
 359
 360
 361
 362
 363
 364
 365
 366
 367
 368
 369
 370
 371
 372
 373
 374
 375
 376
 377
 378
 379
 380
 381
 382
 383
 384
 385
 386
 387
 388
 389
 390
 391
 392
 393
 394
 395
 396
 397
 398
 399
 400
 401
 402
 403
 404
 405
 406
 407
 408
 409
 410
 411
 412
 413
 414
 415
 416
 417
 418
 419
 420
 421
 422
 423
 424
 425
 426
 427
 428
 429
 430
 431
 432
 433
 434
 435
 436
 437
 438
 439
 440
 441
 442
 443
 444
 445
 446
 447
 448
 449
 450
 451
 452
 453
 454
 455
 456
 457
 458
 459
 460
 461
 462
 463
 464
 465
 466
 467
 468
 469
 470
 471
 472
 473
 474
 475
 476
 477
 478
 479
 480
 481
 482
 483
 484
 485
 486
 487
 488
 489
 490
 491
 492
 493
 494
 495
 496
 497
 498
 499
 500
 501
 502
 503
 504
 505
 506
 507
 508
 509
 510
 511
 512
 513
 514
 515
 516
 517
 518
 519
 520
 521
 522
 523
 524
 525
 526
 527
 528
 529
 530
 531
 532
 533
 534
 535
 536
 537
 538
 539
 540
 541
 542
 543
 544
 545
 546
 547
 548
 549
 550
 551
 552
 553
 554
 555
 556
 557
 558
 559
 560
 561
 562
 563
 564
 565
 566
 567
 568
 569
 570
 571
 572
 573
 574
 575
 576
 577
 578
 579
 580
 581
 582
 583
 584
 585
 586
 587
 588
 589
 590
 591
 592
 593
 594
 595
 596
 597
 598
 599
 600
 601
 602
 603
 604
 605
 606
 607
 608
 609
 610
 611
 612
 613
 614
 615
 616
 617
 618
 619
 620
 621
 622
 623
 624
 625
 626
 627
 628
 629
 630
 631
 632
 633
 634
 635
 636
 637
 638
 639
 640
 641
 642
 643
 644
 645
 646
 647
 648
 649
 650
 651
 652
 653
 654
 655
 656
 657
 658
 659
 660
 661
 662
 663
 664
 665
 666
 667
 668
 669
 670
 671
 672
 673
 674
 675
 676
 677
 678
 679
 680
 681
 682
 683
 684
 685
 686
 687
 688
 689
 690
 691
 692
 693
 694
 695
 696
 697
 698
 699
 700
 701
 702
 703
 704
 705
 706
 707
 708
 709
 710
 711
 712
 713
 714
 715
 716
 717
 718
 719
 720
 721
 722
 723
 724
 725
 726
 727
 728
 729
 730
 731
 732
 733
 734
 735
 736
 737
 738
 739
 740
 741
 742
 743
 744
 745
 746
 747
 748
 749
 750
 751
 752
 753
 754
 755
 756
 757
 758
 759
 760
 761
 762
 763
 764
 765
 766
 767
 768
 769
 770
 771
 772
 773
 774
 775
 776
 777
 778
 779
 780
 781
 782
 783
 784
 785
 786
 787
 788
 789
 790
 791
 792
 793
 794
 795
 796
 797
 798
 799
 800
 801
 802
 803
 804
 805
 806
 807
 808
 809
 810
 811
 812
 813
 814
 815
 816
 817
 818
 819
 820
 821
 822
 823
 824
 825
 826
 827
 828
 829
 830
 831
 832
 833
 834
 835
 836
 837
 838
 839
 840
 841
 842
 843
 844
 845
 846
 847
 848
 849
 850
 851
 852
 853
 854
 855
 856
 857
 858
 859
 860
 861
 862
 863
 864
 865
 866
 867
 868
 869
 870
 871
 872
 873
 874
 875
 876
 877
 878
 879
 880
 881
 882
 883
 884
 885
 886
 887
 888
 889
 890
 891
 892
 893
 894
 895
 896
 897
 898
 899
 900
 901
 902
 903
 904
 905
 906
 907
 908
 909
 910
 911
 912
 913
 914
 915
 916
 917
 918
 919
 920
 921
 922
 923
 924
 925
 926
 927
 928
 929
 930
 931
 932
 933
 934
 935
 936
 937
 938
 939
 940
 941
 942
 943
 944
 945
 946
 947
 948
 949
 950
 951
 952
 953
 954
 955
 956
 957
 958
 959
 960
 961
 962
 963
 964
 965
 966
 967
 968
 969
 970
 971
 972
 973
 974
 975
 976
 977
 978
 979
 980
 981
 982
 983
 984
 985
 986
 987
 988
 989
 990
 991
 992
 993
 994
 995
 996
 997
 998
 999
 1000
 1001
 1002
 1003
 1004
 1005
 1006
 1007
 1008
 1009
 1010
 1011
 1012
 1013
 1014
 1015
 1016
 1017
 1018
 1019
 1020
 1021
 1022
 1023
 1024
 1025
 1026
 1027
 1028
 1029
 1030
 1031
 1032
 1033
 1034
 1035
 1036
 1037
 1038
 1039
 1040
 1041
 1042
 1043
 1044
 1045
 1046
 1047
 1048
 1049
 1050
 1051
 1052
 1053
 1054
 1055
 1056
 1057
 1058
 1059
 1060
 1061
 1062
 1063
 1064
 1065
 1066
 1067
 1068
 1069
 1070
 1071
 1072
 1073
 1074
 1075
 1076
 1077
 1078
 1079
 1080
 1081
 1082
 1083
 1084
 1085
 1086
 1087
 1088
 1089
 1090
 1091
 1092
 1093
 1094
 1095
 1096
 1097
 1098
 1099
 1100
 1101
 1102
 1103
 1104
 1105
 1106
 1107
 1108
 1109
 1110
 1111
 1112
 1113
 1114
 1115
 1116
 1117
 1118
 1119
 1120
 1121
 1122
 1123
 1124
 1125
 1126
 1127
 1128
 1129
 1130
 1131
 1132
 1133
 1134
 1135
 1136
 1137
 1138
 1139
 1140
 1141
 1142
 1143
 1144
 1145
 1146
 1147
 1148
 1149
 1150
 1151
 1152
 1153
 1154
 1155
 1156
 1157
 1158
 1159
 1160
 1161
 1162
 1163
 1164
 1165
 1166
 1167
 1168
 1169
 1170
 1171
 1172
 1173
 1174
 1175
 1176
 1177
 1178
 1179
 1180
 1181
 1182
 1183
 1184
 1185
 1186
 1187
 1188
 1189
 1190
 1191
 1192
 1193
 1194
 1195
 1196
 1197
 1198
 1199
 1200
 1201
 1202
 1203
 1204
 1205
 1206
 1207
 1208
 1209
 1210
 1211
 1212
 1213
 1214
 1215
 1216
 1217
 1218
 1219
 1220
 1221
 1222
 1223
 1224
 1225
 1226
 1227
 1228
 1229
 1230
 1231
 1232
 1233
 1234
 1235
 1236
 1237
 1238
 1239
 1240
 1241
 1242
 1243
 1244
 1245
 1246
 1247
 1248
 1249
 1250
 1251
 1252
 1253
 1254
 1255
 1256
 1257
 1258
 1259
 1260
 1261
 1262
 1263
 1264
 1265
 1266
 1267
 1268
 1269
 1270
 1271
 1272
 1273
 1274
 1275
 1276
 1277
 1278
 1279
 1280
 1281
 1282
 1283
 1284
 1285
 1286
 1287
 1288
 1289
 1290
 1291
 1292
 1293
 1294
 1295
 1296

1 module, based on the degree-day method. Comparison of
2 its performance against that of an energy balance model
3 can be found in Chaponnière (2005).

4 It is worthwhile mentioning that, in contrast to snow
5 surface, the runoff is not strongly affected by SNO₁₀₀
6 because its value is low in the area of interest, where
7 there is no vegetation and a low surface rugosity. Con-
8 sequently, the use of either the default or the cali-
9 brated equation has little impact on the runoff simulation.
10 Increased accuracy in the simulation of this intermedi-
11 ate process does not affect the runoff simulation quality
12 significantly.

15 DISCUSSION

16 The watershed studied here is complex, and different
17 storage and redistribution processes ('intermediate pro-
18 cesses') contribute to the streamflow signal at the outlet.
19 Significant surface runoff is expected on the steep slopes
20 and shallow soils during intense rain events. Rapid over-
21 land flow contributes to streamflow within a few hours
22 to a few days (depending on the location and intensity of
23 the storm). In terms of 'slow processes', the groundwater
24 and snowmelt contribute to streamflow at a time scale of
25 several weeks to months (depending on climatic condi-
26 tions for the snow). There are thus at least three major
27 contributions to streamflow, which are characterized by
28 seemingly distinctive temporal signatures. The modelling
29 exercise shows that the processes that might present high
30 equifinality issues include soil, groundwater and snow
31 modules. The problems inherent to the evaluation of
32 soil parameters have not been addressed here, but could
33

34 definitely provide some important insight in the rapid-
35 streamflow response of the basin. The groundwater and
36 snowfall/snowmelt processes have been analysed in more
37 detail in order to estimate how realistically these intermedi-
38 ate processes are simulated by the model. These pro-
39 cesses have similar temporal signatures on the streamflow
40 time-series and are intercorrelated; it is thus important
41 to be able to analyse how realistically they are modelled.
42 We found that the algorithms used in SWAT to compute
43 the groundwater contribution to streamflow are not appro-
44 priate. Modelling them as a simple constant contribution
45 would be enough in our zone of interest. Regarding the
46 snow cover, it is fairly accurately reproduced by the
47 model once the distribution equation is calibrated.

48 The modelling presented in this study considered
49 three HRUs for the whole watershed. This division
50 was chosen based on geomorphological observations and
51 the analysis of soil and geological maps. It reflects the
52 major geomorphological units of the watershed, and
53 the number of units seemed reasonable to us given
54 the lack of information on the hydrological cycle of the
55 basin. However, this number is low and does not reflect
56 the complexity of the watershed. Considering a higher
57 number of HRUs would be more realistic but would
58 bring up severe equifinality issues. Additional details in
59 the modelling would first require a better hydrological
60 characterization of the watershed.

61 Additionally, this study took place in a semi-arid envi-
62 ronment where high water losses are expected: via evap-
63 otranspiration for the vegetation and via sublimation for
64 snow. Snow penitentes (pointed peaks of hard snow)
65 are signs of a high sublimation rate. On the southern slopes
66 of the High Atlas, Schulz and de Jong (2004) observed

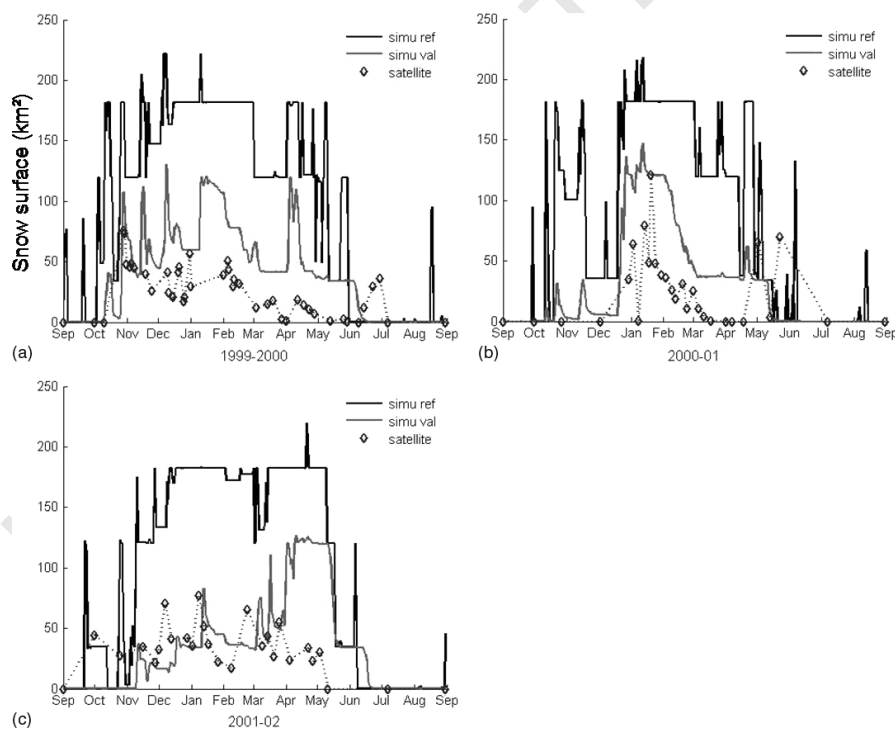


Figure 14. Estimated surface snow temporal profiles (km²) by satellite images ('satellite', diamond symbols), reference SWAT simulation ('simu ref', continuous line) and calibrated SWAT simulation ('simu opt', dashed line) for (a) year 1999–2000, (b) year 2000–2001 and (c) year 2001–2002

penitents. Modelling snow ablation with an energy balance model, they found an average 44% of snow removed by sublimation. The modelling was conducted at two sites located at 3250 m and 2960 m during 39 days and 20 days respectively. Sublimation is thus an important component to be taken into account. However, we believe the sublimation rate in the Rehraya watershed to be less important because northern slopes experience less arid climatic conditions than southern slopes and because we observed only a few penitentes above 4000 m (whereas Schulz and de Jong (2004) observe more and at lower elevation). In SWAT, evapotranspiration is simulated with the Penman equation and potential evaporation applies directly to snow, which sublimates to fulfil the demand (which equals half the potential evaporation) unless the quantity of snow is below a given threshold. The impact on the runoff retrieval accuracy of using *in situ* climatic data or generated climatic data from long-term historical mean is low, as demonstrated by Chaponnière (2005). However, the potential and actual evapotranspiration have not been compared with ground measurements via scintillometry, for example. Real evapotranspiration of the dense irrigated agricultural vegetation in the valleys needs a better characterization. Andréassian *et al.* (2004) discuss the impact of potential evaporation errors on model efficiency and provide a very complete literature on this issue. Further investigation of this compartment in the Rehraya watershed would definitely provide a valuable input.

CONCLUSIONS

In southern Morocco, large irrigated districts rely on the water coming from the Atlas Mountains. However, water transfer mechanisms from the mountains down to the plains remain poorly understood. An understanding of these mechanisms is of crucial importance for developing management strategies that ensure the sustainability of irrigation under the currently changing environment. In this paper, the water cycle of a poorly instrumented semi-arid mountainous watershed is simulated. The main aim of this work was to analyse whether optimal parameters sets (calibrated using a cost-function based on the streamflow data) are consistent with a realistic process representation or whether they only reflect parameter intercorrelation. SWAT was implemented for the Rehraya watershed. We found that evaluating the model performance by comparing simulated and observed streamflow only is insufficient, especially when parameter intercorrelation is identified. The analysis of best-fit parameter ranges when tuning an increasing number of parameters shows that compensation effects seem to take place in the soil, the groundwater and the snow modules, i.e. for the quickest and the slowest water transfer processes. The evaluation of soil parameters was not addressed in the present study. To be able to separate the influence of the slowest processes on streamflow accurately, especially during low flows, special tools and methodologies

tailored to the situation (remote access, low level of instrumentation, high variability, etc.) have been used. A geochemical analysis was performed for the groundwater module and a remote-sensing methodology was developed for the snow module. The outputs from the model were compared with the 'observations' corresponding to the individual processes, and the quality of the simulation of the process was assessed. The geochemical method shows that the groundwater contribution to streamflow of this watershed is low and constant (equal to low flow) throughout the year, whereas the model simulates this contribution as a portion of the total streamflow, thus following the general streamflow pattern. As for the snow module, the simulated evolution of snow cover is compared with the satellite-retrieved snow extent. The distribution equation of the model used to compute snow cover is adapted to the watershed. We showed, on the one hand, that the groundwater module was not appropriate for our mountain watershed and, on the other hand, that simulated snow distribution better reflects the observed patterns after calibration of the snow distribution equation. To be taken further, the study would need to analyse soil parameters, which would provide valuable insight into the rapid-streamflow response of the basin. Also, a detailed analysis of the evapotranspiration module would bring valuable inputs. Benefiting from the information on different individual processes, modification of the model would lead to realistic and fully validated modelling. The multidisciplinary approach adopted here to increase the insight into the hydrological processes is supported by the hydrological community (Sivapalan *et al.*, 2003), but is still uncommon. More effort should be dedicated to these kinds of approach, since they give access to information that is not available in major parts of the world where measurement networks do not exist.

ACKNOWLEDGEMENTS

We would like to thank J. L. Probst from the Laboratoire de Mécanismes de Transfert en Géologie (LMTG, Toulouse, France), who provided his expertise and advice, together with access to the geochemical laboratory, as well as S. Elouaddat from Agence de Bassin du Haouz-Tensift (ABHT, Marrakech, Morocco), who facilitated the acquisition of the hydro-meteorological data on the Rehraya watershed. We gratefully acknowledge support from the research projects SUDMED and EU-funded project IRRIMED and Pleiades. We also extend our thanks to Dr Lahaussais-Bartosik for her review of the English. Finally, we wish to acknowledge the comments of anonymous reviewers, which greatly contributed to improving the manuscript.

REFERENCES

- Ambrose B. 1999. *La Dynamique du Cycle de l'Eau dans un Bassin Versant: Processus, Facteurs, Modèles*. Editions HGA: Bucharest.
- Andréassian V, Perrin C, Michel C. 2004. Impact of imperfect potential evapotranspiration knowledge on the efficiency and parameters of watershed models. *Journal of Hydrology* **286**: 19–35.

- 1 Arnold JG, Allen PM. 1996. Estimating hydrological budgets for three
2 Illinois watersheds. *Journal of Hydrology* **176**: 57–77.
- 3 Arnold JG, Allen PM, Bernhardt G. 1993. A comprehensive surface–
4 groundwater flow model. *Journal of Hydrology* **142**: 42–69.
- 5 Batchelor C, Cain J, Farquharson F, Roberts J. 1998. *Improving Water
6 Utilization from a Catchment Perspective*. SWIM Paper 4. International
7 Water Management Institute: Colombo, Sri Lanka.
- 8 Beven KJ. 1996. Equifinality and uncertainty in geomorphological
9 modelling. In *The Scientific Nature of Geomorphology*, Rhoads BL,
10 Thorn CE (eds). Wiley: Chichester; 289–313.
- 11 Beven KJ, Quinn PF. 1994. Similarity and scale effects in the water
12 balance of heterogeneous area. In *The Balance of Water—Present and
13 Future*, Keane T, Daly E (eds). AGMET: Dublin.
- 14 Chaponnière A. 2005. *Fonctionnement hydrologique d'un bassin versant
15 montagneux semi-aride. Cas du bassin versant du Rehraya (Haut Atlas
16 marocain)*. PhD dissertation, Institut National Agronomique, Paris,
17 France.
- 18 Chaponnière A, Maisongrande P, Duchemin B, Hanich L, Boulet G,
19 Halouat S, Escadafal R. 2005. A combined high and low spatial
20 resolution approach for mapping snow covered area in the Atlas
21 Mountain. *International Journal of Remote Sensing* **26**: 2755–2777.
- 22 Chehbouni A, Watts C, Lagouarde J-P, Kerr YH, Rodriguez J-C, Bon-
23 nefond J-M, Santiago F, Dedieu G, Goodrich DC, Unkrich C. 2000.
24 Estimation of heat and momentum fluxes over complex terrain using a
25 large aperture scintillometer. *Journal of Agricultural and Forest Meteorology* **105**: 215–226.
- 26 Chehbouni A, Escadafal R, Boulet G, Duchemin B, Simonneaux V,
27 Dedieu G, Mougnot B, Khabba S, Kharrou H, Merlin O,
28 Chaponnière A, Ezzahar J, Erraki S, Hoedjes J, Hadria R, Abourida A,
29 Cheggour A, Raïbi F, Hanich L, Guemouria N, Chehbouni Ah,
30 Olliso A, Jacob F, Sobrino J. 2006. Integrated modeling and remote
31 sensing approach, toward a sustainable management of water resources
32 in a semi-arid region: the SUDMED project. *International Journal of
33 Remote Sensing* •submitted for publication.
- 34 Conan C, Bouraoui F, de Marsily G, Turpin N, de Marsily G,
35 Bidoglio G. 2003. Modeling flow and nitrate fate at catchment scale in
36 Brittany (France). *Journal of Environmental Quality* **32**: 2026–2032.
- 37 Ezzahar J, Chehbouni A, Hoedjes JCB, Chehbouni Ah. 2007. On the
38 application of scintillometry over heterogeneous grids. *Journal of
39 Hydrology* **334**: 493–501.
- 40 Hernandez M, Miller S, Goodrich DC, Goff BF, Kepner WG, Edmonds
41 CM, Jones KB. 2000. Modeling runoff response to land cover and
42 rainfall spatial variability in semi-arid watersheds. *Environmental
43 Monitoring and Assessment* **64**: 285–298.
- 44 Holko L, Lepistö A. 1997. Modelling the hydrological behaviour of a
45 mountain catchment using TOPMODEL. *Journal of Hydrology* **196**:
46 361–377.
- 47 Idir S, Probst A, Viville D, Probst JL. 1999. Contribution des surfaces
48 saturées et des versants aux flux d'eau et d'éléments exportés en
49 période de crue: traçage à l'aide du carbone organique dissous et de
50 la silice. Cas du petit bassin versant du Strengbach (Vosges, France).
51 *Earth and Planetary Science* **328**: 89–96.
- 52 •Klemes V. 1990. Foreword. In *Hydrology of Mountainous Areas*,
53 Molnár L (ed.). IAHS Publication No. 190. IAHS Press: Wallingford.
- 54 Krishna AP. 2005. Snow and glacier cover assessment in the
55 high mountains of Sikkim Himalaya. *Hydrological Processes* **19**:
56 2375–2383.
- 57 Mutti RS, Wurbs RA. 2002. Scale-dependent soil and climate
58 variability effects on watershed water balance of the SWAT model.
59 *Journal of Hydrology* **256**: 264–285.
- 60 Nash J, Sutcliffe J. 1970. River flow forecasting through conceptual
61 models, 1. A discussion of principles. *Journal of Hydrology* **10**:
62 282–290.
- 63 Pellenq J, Boulet G. 2004. A methodology to test the pertinence of
64 remote-sensing data assimilation into vegetation models for water and
65 energy exchange at the land surface. *Agronomie* **24**: 197–204. DOI:
66 10.1051/agro:2004017.
- 67 Pilgrim DH, Huff DD, Steele D. 1979. Use of specific conductance and
68 contact time relations for separating flow components in storm runoff.
69 *Water Resources Research* **15**: 329–339.
- 70 Pinder GF, Jones JF. 1969. Determination of the ground-water
71 component of peak discharge from the chemistry of total runoff. *Water
72 Resources Research* **5**: 438–445.
- 73 Probst JL. 1992. *Géochimie et hydrologie de l'érosion continentale.
74 Mécanismes, bilan global actuel et fluctuations au cours des 500
75 derniers millions d'années*. *Sciences Géologiques Mémoire* 94,
76 Université Louis Pasteur/Centre National de la Recherche Scientifique:
77 Strasbourg.
- 78 Probst A, Dambrine E, Viville D, Fritz B. 1990. Influence of acid
79 atmospheric inputs on surface water chemistry and mineral fluxes in
80 a declining spruce stand within a small granitic catchment (Vosges
81 Massif, France). *Journal of Hydrology* **116**: 101–124.
- 82 Putty MRY, Prasad R. 2000. Understanding runoff processes using a
83 watershed model—a case study in the Western Ghats in South India.
84 *Journal of Hydrology* **228**: 215–227.
- 85 Rodda JC. 1994. Mountains—a hydrological paradox or paradise?
86 *Beiträge zur Hydrologie der Schweiz* **35**: 41–51.
- 87 Schmutge TJ, Jackson TJ. 1996. Soil moisture variability. In *Scaling
88 up in Hydrology Using Remote Sensing*, Stewart JB, Engman ET,
89 Feddes RA, Kerr Y (eds). Wiley: Chichester; 183–192.
- 90 Schulz O, de Jong C. 2004. Snowmelt and sublimation: field experiments
91 and modelling in the High Atlas Mountains of Morocco. *Hydrology and
92 Earth System Sciences* **8**: 1076–1089.
- 93 Sivapalan M, Takeuchi K, Franks SW, Gupta VK, Karambiri H, Lak-
94 shmi V, Liang X, McDonnell JJ, Mendiondo EM, O'Connell PE,
95 Oki T, Pomeroy JW, Schertzer D, Uhlenbrook S, Zehe E. 2003. IAHS
96 Decade on Predictions in Ungauged Basins (PUB), 2003–2012: shap-
97 ing an exciting future for the hydrological sciences. *Hydrological
98 Sciences Journal/Journal des Sciences Hydrologiques* **48**: 857–880.
- 99 Smakhtin VU. 2001. Low flow hydrology: a review. *Journal of Hydrology*
100 **240**: 147–186.
- 101 Sophocleous MA, Koelliker JK. 1999. Integrated numerical modeling for
102 basin-wide water management: the case of the Rattlesnake Creek basin
103 in south-central Kansas. *Journal of Hydrology* **214**: 179–196.
- 104 Sorooshian S, Gupta VK. 1983. Automatic calibration of conceptual
105 rainfall–runoff models: the question of parameter observability and
106 uniqueness. *Water Resources Research* **19**: 260–268.
- 107 Tani M. 1996. An approach to annual water balance for small
108 mountainous catchments with wide spatial distributions of rainfall and
109 snow water equivalent. *Journal of Hydrology* **183**: 205–225.
- 110 Tardy Y, Bustillo V, Boeglin JL. 2004. Geochemistry applied to the
111 watershed survey: hydrograph separation, erosion and soil dynamics. A
112 case study: the basin of the Niger River, Africa. *Applied Geochemistry*
113 **19**: 469–518.
- 114 Weingartner R, Barben M, Spreafico M. 2003. Floods in mountain
115 areas—an overview based on examples from Switzerland. *Journal of
116 Hydrology* **282**: 10–24.
- 117 Winiger M, Gumpert M, Yamout H. 2005. Karakorum–Hindukush—
118 western Himalaya: assessing high-altitude water resources. *Hydrolog-
119 ical Processes* **19**: 2329–2338.